A physically meaningful new approach to parametric excitation and attenuation of oscillations in nonlinear systems

Eugene I. Butikov

St. Petersburg State University, St. Petersburg, Russia

Abstract

Parametric excitation of a nonlinear physical pendulum by modulation of its moment of inertia is analyzed in terms of physics as an example of the suggested approach. The modulation is provided by a redistribution of auxiliary masses. The system is investigated both analytically and with the help of computer simulations. The threshold and other characteristics of parametric resonance are found and discussed in detail. The role of nonlinear properties of the physical system in restricting the resonant swinging is emphasized. Phase locking between the drive and oscillations of the pendulum, and the phenomenon of parametric autoresonance are investigated. The boundaries of parametric instability are determined as functions of the modulation depth and the quality factor. The feedback providing active optimal control of amplification and attenuation of oscillations is analyzed. An effective method of suppressing undesirable rotary oscillations of suspended constructions is suggested.

Keywords: parametric resonance, active control, phase locking, autoresonance, bifurcations, instability ranges.

1 Introduction: Parametric resonance

According to conventional classification of oscillations by their method of excitation (see, for example, [1]), oscillations are called parametric if they are excited by a periodic variation of some parameter of the oscillatory system. When the oscillations caused by a periodic modulation acquire an increasing character, the phenomenon is called parametric resonance. In conditions of parametric resonance, the state of equilibrium becomes unstable: the system leaves it executing oscillations with progressively increasing amplitude.

In particular, a pendulum can be excited parametrically by a given vertical motion of its suspension point. In the non-inertial frame of reference associated with the pivot, such forcing of the pendulum is equivalent to periodic modulation of the gravitational field. This apparently simple physical system exhibits a surprisingly vast variety of possible regular and chaotic motions. Hundreds of texts and papers are devoted to investigation of the pendulum with vertically oscillating pivot: see, for example, Refs. [2]–[3] and references therein. A widely known curiosity in the behavior of an ordinary rigid planar pendulum whose pivot is forced to oscillate along the vertical line is the dynamic stabilization of its inverted position, occurring when the driving amplitude and frequency lie in certain intervals (see, for example, Refs. [3]–[6]).

Another familiar method of parametric excitation of a pendulum consists in a periodic variation of its length. In many textbooks and papers (see, for example, Refs. [7]–[13]), such a system is considered as a simple model of a playground swing. This mode of parametric pumping is often used as a lecture demonstration to illustrate the phenomenon of parametric resonance: A thread with a bob hanging on its end passes through a little ring fixed immovably in a support. The other end of the thread is pulled by hand through some small distance each time the swinging bob crosses the middle position, and then released to its previous length each time the bob reaches the utmost deflection.

The method of parametric pumping of the pendulum by periodic variation of its length was used already in the Middle Ages. A fascinating description of such exotic example can be found in Ref. [14], p. 27, and Ref. [15]. In Spain, in the cathedral of a northern town Santiago de Compostela, there is a famous *O Botafumeiro*, a very large incense burner suspended by a long rope, which can swing through a huge arc. The censer is pumped by periodically shortening and lengthening the rope as it is wound up and then down around the rollers supported high above the floor of the nave. The pumping action is carried out by a squad of priests, each holding a rope that is a strand of the main rope that goes from the pendulum to the rollers and back down to near the floor. The priests periodically pull on the ropes in response to orders from the chief verger of the cathedral. One of the more terrifying aspects of the pendulum's motion is the fact that the amplitude of its swing is very large, and it passes through the bottom of its arc with a high velocity, spewing smoke and flames.

In this paper we explore analytically and by numerical simulations another method of parametric excitation and, more generally, a method of oscillation control, which can be applied to an arbitrary physical pendulum. The suggested method is based on periodic modulation of the inertia moment. We have already used this idea earlier for explanation the basics of parametric resonance in a simple linear system [16], namely, in a torsion spring oscillator, similar to the balance device of a mechanical watch (see Figure 1).

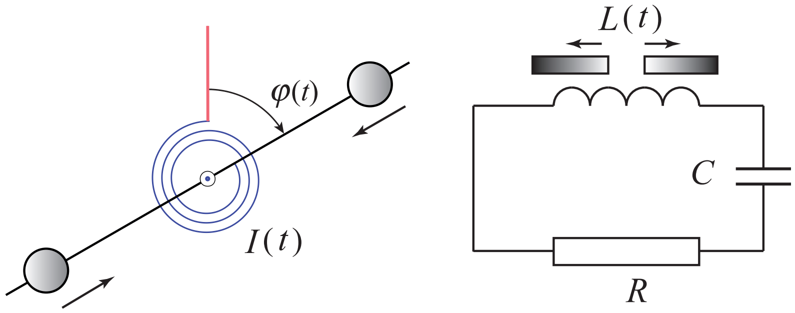

Figure 1: Schematic image of the torsion spring oscillator with a rotor whose moment of inertia is forced to vary periodically (left), and an analogous *LCR*-circuit with a coil whose inductance is modulated by moving periodically an iron core in and out of the coil (right).

The system consists of a rigid rod that can rotate about an axis that passes through its center. Two identical weights are balanced on the rod. An elastic spiral spring is attached to the rod. The other end of the spring is fixed. When the rod is turned about its axis, the spring flexes. The restoring torque of the spring is proportional to the angular displacement of the rotor from the equilibrium position. After a disturbance, the rotor executes natural harmonic torsional oscillations. A similar mechanical system was investigated later in [17] by another method based on an analysis of the behavior of Floquet multipliers.

We assume that the weights can be shifted simultaneously along the rod in opposite directions into other symmetrical positions so that the rotor as a whole remains balanced. However, its moment of inertia is changed by such displacements of the weights.

When the weights are shifted toward or away from the axis, the moment of inertia decreases or increases, respectively. As the moment of inertia of the rotor is changed, so also is the natural frequency of its oscillation. Thus, the moment of inertia of the rotor is the parameter to be modulated in this system. This physical system is ideal for investigation of parametric resonance and has several advantages in understanding its counterintuitive features because it gives a very clear example of the phenomenon in a linear mechanical system. All peculiarities of parametric excitation in this linear system can be completely explained and exhaustively investigated by rather modest mathematical means even quantitatively (see [16], [18]–[19]).

A similar method of modulation can be applied to a nonlinear system such as a physical pendulum, in which case the restoring torque is proportional to the sine of the deflection angle φ (see Figure 2, *a* or *b*). The two additional weights located at equal distances from the pivot can be shifted simultaneously along the rod in opposite directions into other symmetrical positions so that the pendulum's center of mass remains at the same distance from the pivot. Hence, the restoring torque of gravity is not influenced by such displacements of the weights. However, the moment of inertia of the physical pendulum about the pivoting axis is changed.

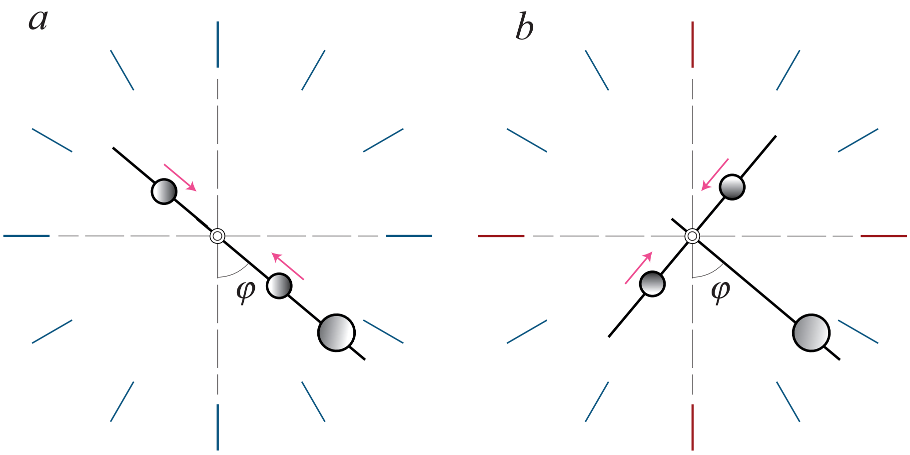

Figure 2: Schematic images of physical pendulums whose moments of inertia are forced to vary periodically by simultaneously shifting the two additional masses in opposite directions. Such motions of the weights are not influential on the restoring torque of gravity.

We emphasize that this simple model is applicable to an arbitrary physical pendulum with additional masses whose reconfiguration changes the moment of inertia: It is not necessary for the pendulum to look like a rigid rod with a heavy bob at its end as shown on the schematic image in Figure 2. The physical model discussed in the paper is also applicable to systems like suspended heavy beams or plates that can execute rotary oscillations about the vertical axis (see Figure 10). Such oscillations can be excited and controlled by periodic reconfigurations of auxiliary masses whose positions influence the central moment of inertia of the suspended body about the vertical axis.

On the basis of the simple model of a nonlinear mechanical system that is suggested in the paper, we demonstrate and explain in terms of physics all specific features characteristic of the behavior of parametrically excited dynamical systems. For the adopted simple excitation mode, many of the calculations necessary for the analysis can be performed analytically on the basis of the conservation laws and equations describing the simple model of the system. Our conclusions about the behavior of the system drawn from the analytical calculations are illustrated by the results of numerical simulations.

In a great majority of papers and monographs, the phenomena associated with parametric excitation and instability are explained in terms of the theory of differential equations with periodic coefficients (Floquet theory, Hill and Mathieu equations). The nature of such papers is predominantly mathematical and actually gives very little insight into the phenomena. It is not always easy to understand the physical essence of the parametric excitation from the general mathematical theory. The physical sense of the investigated phenomena is buried deeply in severe and non-transparent mathematics, which could turn out to be abstract and very complicated for physicists and engineers. Moreover, the issues regarding control of oscillations via variation of a parameter remain usually beyond the scope of investigation.

The mainstream of the present work on the pendulum with modulated inertia moment refers to the physics of the parametric excitation including the possibility of effectively controlling vibrations. We are trying to give clear qualitative physical explanations of the phenomena relying on Newton's laws and conservation principles, and to obtain in this way even quantitative rigorous results whenever possible. It occurs that this is possible without the usage of the Floquet theory, infinite Hill's determinants and perturbation methods. The differential equations are used only when they are actually needed (say, to determine quantitatively the boundaries of the instability domains).

The paper is organized as follows. In Section 2 we discuss the forces exerted on the mass that is sliding along a rotating body. Section 3 explains how and under what conditions the forces of reaction can cause parametric swinging of the pendulum. In Section 4 an average natural frequency that depends on the depth of modulation is introduced. The threshold of parametric resonance is calculated in Section 5 on the basis of energy considerations. In Section 6, we discuss how the feedback can be used for amplification or attenuation of oscillations, and for active control of the amplitude, including parametric suppressing of harmful vibrations. Phenomenon of phase locking, parametric autoresonance and bifurcations are described in Section 7. Ranges of parametric instability are calculated in Sections 8 – 10. Finally, a concluding discussion is presented in Section 11.

2 Effects caused by variations of the moment of inertia

Next we explain in physical terms why and how the forced radial movement of the additional masses influences the angular velocity of the pendulum's rotation about the axis. To do this, we use Newton's laws for understanding the forces that cause radial movements of auxiliary masses. First of all we need to know the acceleration of the sliding mass with respect to the inertial frame of reference (laboratory frame). When the pendulum rotates with a constant angular velocity ω (see Figure 3), and a weight of mass M is sliding along the rod attached to the pendulum with some velocity $\mathbf{v}_\mathrm{r}$ relative to the rod, the acceleration $\mathbf{a}_\mathrm{abs}$ of the weight in the inertial reference frame can be represented as a sum of the following three terms (see, for example, Refs. [20], [21]):

$$\mathbf{a}_\mathrm{abs} = \mathbf{a}_\mathrm{rel} + \mathbf{a}_\mathrm{cp} + \mathbf{a}_\mathrm{Cor}, \tag{1}$$

where $\mathbf{a}_\mathrm{rel}$ is acceleration of the sliding weight relative to the rod, $\mathbf{a}_\mathrm{cp} = \omega \times [\omega \times \mathbf{r}]$ is the centripetal acceleration directed toward the axis of rotation, and $\mathbf{a}_\mathrm{Cor} = 2\omega \times \mathbf{v}_\mathrm{r}$ is the Coriolis' acceleration directed perpendicularly to the rotating rod.

Further on we consider the forces exerted on a sliding weight by the source that makes the weight shifting along the rod. Both $\mathbf{a}_\mathrm{rel}$ and $\mathbf{a}_\mathrm{cp}$ are directed along the rod. Hence the corresponding components $M\mathbf{a}_\mathrm{rel}$ and $M\mathbf{a}_\mathrm{cp}$ of the force exerted on the weight that are responsible for these accelerations are also directed radially. Equal and opposite forces of reaction are also radial, and hence are not influential on the angular velocity ω of the pendulum's rotation. But

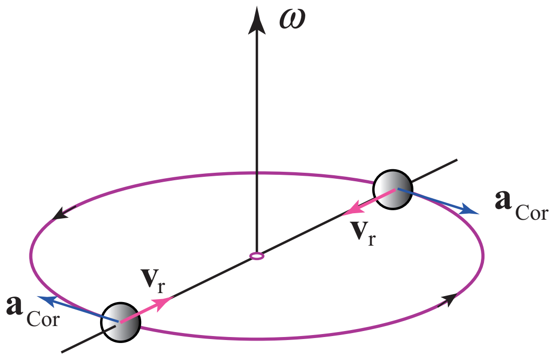

Figure 3: 3d-schematic image of the two additional masses moving in opposite directions with radial velocity $\mathbf{v}_\mathrm{r}$ along the rod that rotates with angular velocity ω. With respect to the inertial reference frame, each of the weights has the Coriolis' acceleration $\mathbf{a}_\mathrm{Cor} = 2\,\omega \times \mathbf{v}_\mathrm{r}$.

the Coriolis' acceleration $\mathbf{a}_\mathrm{Cor} = 2\omega \times \mathbf{v}_\mathrm{r}$ is perpendicular to the rod (see Figure 3), and so is the corresponding component $M\mathbf{a}_\mathrm{Cor}$ of the force exerted on the weight. According to Newton's third law, equal and opposite force of reaction is applied to the rod. It is just this force of reaction exerted on the rod that is responsible for the change in angular velocity of the pendulum. The pair of these forces of reaction creates a torque that influences the angular velocity ω of the pendulum. From Figure 3 we can clearly see that due to these forces, directed oppositely to vectors $\mathbf{a}_\mathrm{Cor}$, the angular velocity ω increases if the weights are drawn inward (toward the axis). Otherwise, if the weights are shifted outward, away from the axis, the rotation slows down and the angular velocity ω decreases.

We note that the above conclusions regarding the change in the angular velocity caused by movements of the additional masses are independent of the direction of rotation: Both at clockwise or counterclockwise rotation the angular velocity grows if the masses are drawn inward, and vice versa.

These same conclusions regarding the effects on rotational motion produced by changing the moment of inertia can be drawn by considering the principle of conservation of the angular momentum: When the moment of inertia decreases, the angular velocity increases, and vice versa. For example, this principle is often applied to understand the mechanics of a figure skaters' spinning or similar phenomena. However, the explanations based on the conservation of the angular momentum, being useful for quantitative analysis, cannot reveal the dynamics of such phenomena, because the forces that cause them remain obscure.

3 Principal parametric resonance at square-wave modulation of the moment of inertia

In this paper, we concentrate on a periodic piecewise constant (square-wave) modulation of the pendulum's moment of inertia. The square-wave modulation provides an alternative and maybe more straightforward way to understand the underlying physics of parametric resonance and to describe it quantitatively in comparison with a smooth (e.g., sinusoidal) modulation of the parameter.

In the case of the square-wave modulation, abrupt, almost instantaneous increments and decrements in the moment of inertia of the pendulum occur sequentially, separated by equal time intervals. We denote these intervals by $T/2$, so that T equals the whole period of the moment of inertia variation (the period of modulation). Let the changes in the moment of inertia I of the pendulum occur between maximal I_1 and minimal I_2 values that equal $I_0(1+m)$ and $I_0(1-m)$, respectively, where I_0 is a mean value of the moment of inertia, and m is the dimensionless quantity called the depth of modulation (or index of modulation), which equals fractional increments and decrements of the modulated parameter.

During the time intervals $(0,\ T/2)$ and $(T/2,\ T)$, the moment of inertia is constant, and the pendulum's motion can be considered as a free oscillation described by a corresponding differential equation. However, the coefficients in this equation are different for the adjacent time intervals $(0,\ T/2)$ and $(T/2,\ T)$:

$$\ddot{\varphi}+2\gamma\dot{\varphi}+\omega_1^2\sin\varphi=0, \quad \omega_1=\frac{\omega_0}{\sqrt{1+m}}, \ 0<t<T/2, \tag{2}$$

$$\ddot{\varphi}+2\gamma\dot{\varphi}+\omega_2^2\sin\varphi=0, \quad \omega_2=\frac{\omega_0}{\sqrt{1-m}}, \ T/2<t<T. \tag{3}$$

Here $\omega_0=\sqrt{g/l_0}$ is the natural frequency of small oscillations for the pendulum with mean equivalent length l_0, and γ is the damping constant characterizing the strength of viscous friction. The linear dependence of drag on velocity is a reasonable approximation for most important applications. We assume for simplicity that the damping constant γ in this model remains the same when the moment of inertia of the pendulum changes, that is, we assume the values of γ in Eqs. (2) and (3) to be equal.

At each time moment $t_n=nT/2$ ($n=1,\ 2,\ \ldots$) of an abrupt change in the moment of inertia of the pendulum, we must make a transition from one of these equations (2)–(3) to the other. During each half-period $T/2$, the motion of the pendulum is a segment of some natural oscillation. An analytical investigation of parametric excitation can be carried out by fitting to one another known solutions to differential equations (2)–(3) for consecutive adjacent time intervals (see Section 8). The graphs of time history and phase trajectories that illustrate this paper are obtained by numerical integration of these nonlinear equations. However, the most interesting peculiarities in behavior of the investigated system can be explained without solving these equations.

The square-wave modulation can produce considerable oscillation of the pendulum if the period and phase of modulation are chosen properly. For example, suppose that the weights are shifted inward (toward the axis of rotation) at an instant at which the pendulum passes through the lower equilibrium position, when its angular velocity reaches a maximum value. While the weights are moved radially, the angular momentum of the pendulum with respect to the pivot remains constant. Thus, the resulting reduction in the moment of inertia is accompanied by an increment in the angular velocity, and the pendulum gains additional energy. The greater the angular velocity, the greater the increment in energy. This additional energy is supplied by the source that forces the weights to move along the rod. On the other hand, if the weights are instantly moved outward, the angular velocity and the energy of the swinging pendulum diminish. The decrease in energy is transferred back to the source.

In order that increments in energy occur regularly and exceed the amounts of energy returned, i.e., in order that, as a whole, the modulation of the moment of inertia regularly feeds the pendulum with energy, the period and the phase of modulation must satisfy certain conditions.

For instance, let the weights be drawn closer and moved apart from one another twice during one mean period of the natural oscillation. The angular velocity increases at the moment the weights come together, and vice versa. Furthermore, let the weights be drawn closer at the instant of maximum angular velocity, so that the pendulum gains as much energy as possible. Then, after a quarter period of the natural oscillation, the weights are moved apart, and this occurs almost at the instant of extreme deflection, when the angular velocity is nearly zero. Therefore this particular motion causes almost no change in the angular velocity and kinetic energy of the pendulum. Thus, modulating the moment of inertia at a frequency twice the mean natural frequency generates the greatest growth of the amplitude, provided that the phase of the modulation is chosen in the way described above. This is the principal (main) parametric resonance.

If the changes of a parameter occur with the above-mentioned periodicity but not abruptly, the influence of these changes on the pendulum's motion is qualitatively quite similar, though the efficiency of the parametric delivery of energy (at the same amplitude of the parametric modulation) is a maximum for the square-wave time dependence, because this form of modulation provides optimal conditions for the transfer of energy to the oscillating system. The case of the sinusoidal modulation of some parameter is important for numerous practical applications. Parametric instability in systems with this kind of modulation has interesting manifestations in quite distant fields of physics, say, in the behavior of coupled nanomechanical shuttles, being responsible for current rectification by spontaneous symmetry breaking [22].

Contrary to ordinary resonance under direct forcing, variations of a parameter cannot excite the system from the state of rest in the equilibrium position. Moreover, in a system with friction parametric resonance occurs only if the amplitude of modulation exceeds some threshold value (see Section 5). But over the threshold friction is unable to restrict the growth of parametric oscillations. In an idealized linear system like the torsion spring oscillator shown in Figure 1, if conditions of parametric resonance are fulfilled and the modulation depth exceeds the threshold, the amplitude grows indefinitely [16].

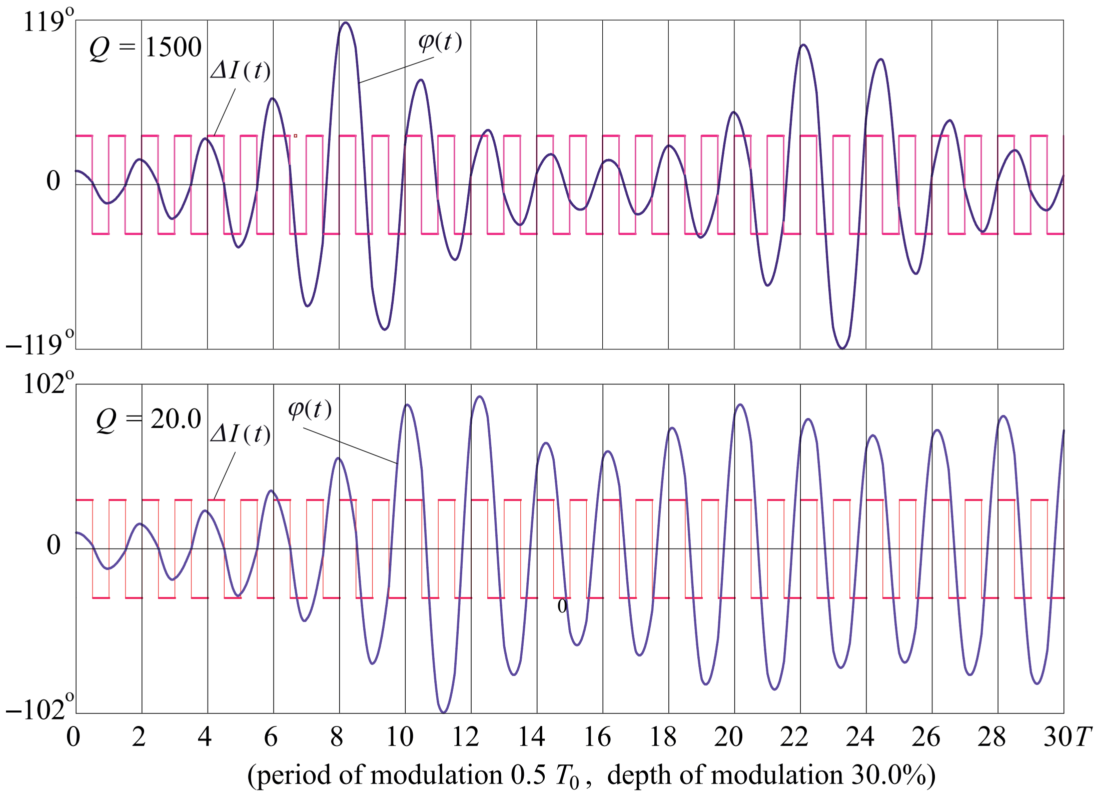

Figure 4: Initial exponential growth of the amplitude of oscillations at parametric resonance of the first order ($n = 1$) under the square-wave modulation, followed by beats.

In a real system the growth of the amplitude at parametric resonance is restricted by nonlinear effects. In a nonlinear system like the pendulum, the natural period depends on the amplitude of oscillations. As the amplitude grows, the natural period of the pendulum becomes longer. However, in the adopted model the drive period (period of modulation) remains constant. If conditions for parametric excitation are fulfilled at small oscillations and the amplitude is growing, the conditions of resonance become violated at large amplitudes. The drive drifts out of phase with the pendulum and the phase relations change gradually to those favorable for the backward transfer of energy from the pendulum to the source of modulation. This causes gradual reduction of the amplitude. The natural period becomes shorter, and conditions for the growth of the amplitude restore. Oscillations acquire the character of beats, as shown in the upper panel of Figure 4. Due to friction these transient beats gradually fade. Fading of the beats goes faster the greater the friction (lower panel of Figure 4), and the amplitude tends to a finite constant value.

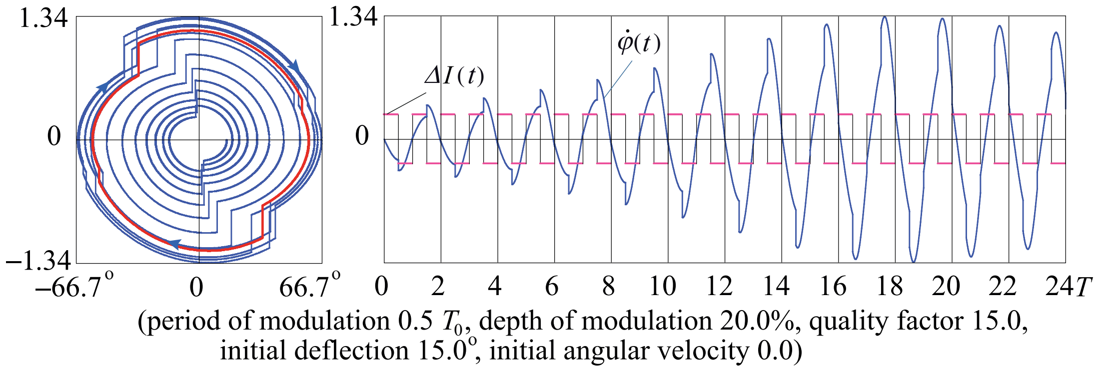

Figure 5: The phase diagram ($\varphi - \dot{\varphi}$ plane, left) and time-dependent graph (right) of angular velocity $\dot{\varphi}(t)$ for the process of resonant growth followed by nonlinear restriction of the amplitude.

Details of the process of resonant growth followed by a nonlinear restriction of the amplitude for parametrically excited pendulum ($T = T_0/2$) with considerable values of the modulation depth (20%) and moderate friction (quality factor $Q = 15$) are shown in Figure 5. The vertical segments of the phase trajectory and of the $\dot{\varphi}(t)$ graph correspond to instantaneous increments and decrements of the angular velocity $\dot{\varphi}$ at the instants at which the weights are shifted inward and outward, respectively. The curved portions of the phase trajectory that spiral in toward the origin correspond to damped natural motions of the pendulum during the intervals between the abrupt shifts of the weights. The initially fast growth of the amplitude (described by the expanding part of the phase trajectory) gradually slows down, because the natural period becomes longer as the amplitude increases. The resonant conditions become violated, and the shifts of the weights occur earlier than required for the resonant growth of oscillations. After reaching some maximum value (66.7° for the case shown in Figure 5), the amplitude decreases and increases several times within a small range approaching slowly its final value (about 59.0° in Figure 5). The initially unwinding spiral of the phase trajectory gradually approaches the closed limit cycle (attractor), whose characteristic shape with four vertical segments can be seen in the left-hand part of Figure 5.

In conditions of parametric resonance the square-wave modulation can produce not only amplification of initially small oscillations of the pendulum, but also attenuation of already existing oscillations. This occurs if the phase of modulation is opposite to the phase that leads to the amplification. Namely, the moment of inertia should be increased by shifting the auxiliary masses outward when the pendulum crosses the equilibrium position, and decreased at extreme deflections (see Figure 6). However, it is impossible to totally suppress the oscillations by

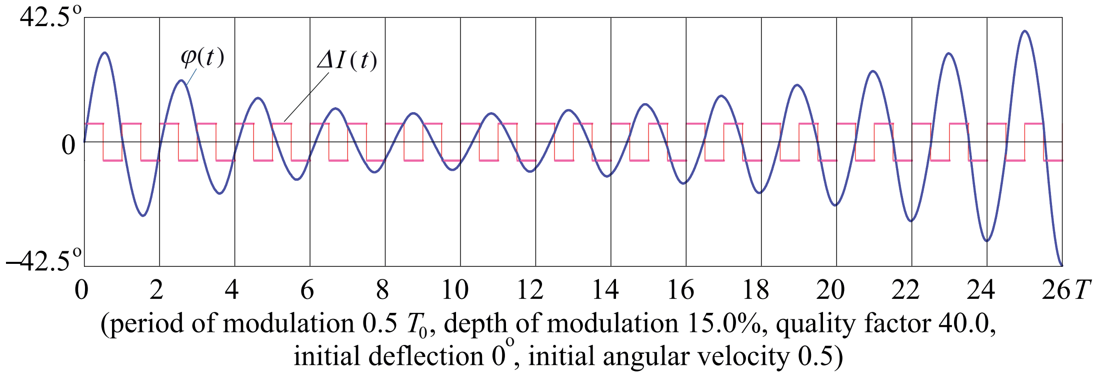

Figure 6: The time-dependent graph of the deflection angle $\varphi(t)$ for the process of parametric attenuation followed by the inevitable resonant growth of the amplitude.

strictly periodic modulation of the parameter: Sooner or later the attenuation will be inevitably replaced by the resonant growth of the amplitude. Undesirable oscillations can be completely suppressed parametrically with the help of a negative feedback (see Section 6).

4 Resonant frequencies and the depth of modulation

Obviously, the energy of the pendulum can increase not only when two full cycles of variation in the parameter occur during one mean natural period, but also when two cycles occur during three, five or any odd number of natural periods (high resonances of odd orders). The delivery of energy, though less efficient, is also possible if two cycles of modulation occur during an even number of natural periods (high resonances of even orders). That is, parametric resonance is possible when one of the following conditions for the frequency ω (or for the period T) of a parameter modulation is approximately fulfilled:

$$\omega = \omega_n = \frac{2\omega_0}{n}, \qquad T = T_n = \frac{nT_0}{2}, \qquad n = 1,\, 2,\, \ldots \tag{4}$$

However, the exact period T of modulation which corresponds to any of the parametric resonances is determined not only by the order n of the resonance, but also by the depth of modulation m. Indeed, for considerable values of the modulation depth m, the notion of a natural period of oscillations needs a more precise definition. Let $T_0 = 2\pi/\omega_0 = 2\pi\sqrt{l_0/g}$ be the period of free oscillation of the physical pendulum when its auxiliary masses are fixed in their middle positions, for which the equivalent length of the pendulum equals l_0. The period is somewhat longer when the weights are displaced further from the axis of rotation: $T_1 = T_0\sqrt{1+m} \approx T_0(1+m/2)$. The period is shorter when the weights are moved closer to the axis: $T_2 = T_0\sqrt{1-m} \approx T_0(1-m/2)$.

It is expedient to define the average natural period $T_{\rm av}$ not as the arithmetic mean of periods T_1 and T_2, but rather as the period that corresponds to the arithmetic mean frequency $\omega_{\rm av} = \frac{1}{2}(\omega_1 + \omega_2)$, where $\omega_1 = 2\pi/T_1$ and $\omega_2 = 2\pi/T_2$. That is, we define $T_{\rm av}$ by the relation:

$$T_{\rm av} = \frac{2\pi}{\omega_{\rm av}} = \frac{2T_1T_2}{T_1+T_2}. \tag{5}$$

Indeed, in order to satisfy the resonant conditions, the increment in the phase of natural oscillations during one cycle of modulation must be equal to π, 2π, 3π, $\ldots$, $n\pi$, $\ldots$. During the first half-cycle, the phase of oscillation increases by $\omega_1 T/2$, and during the second half-cycle— by $\omega_2 T/2$. Consequently, instead of the approximate condition expressed by Eq. (4), we obtain:

$$\frac{\omega_1+\omega_2}{2}T = n\pi, \quad \text{or} \quad T = T_n = n\frac{\pi}{\omega_{\rm av}} = n\frac{T_{\rm av}}{2}. \tag{6}$$

Thus, for a parametric resonance of some definite order n, the condition for exact tuning is $T = nT_{\rm av}/2$, where $T_{\rm av}$ is defined by Eq. (5). For small and moderate values of m it is possible to use approximate expressions for the average natural frequency and period:

$$\omega_{\rm av} = \frac{\omega_0}{2}\left(\frac{1}{\sqrt{1+m}}+\frac{1}{\sqrt{1-m}}\right) \approx \omega_0\left(1+\frac{3}{8}m^2\right), \quad T_{\rm av} \approx T_0\left(1-\frac{3}{8}m^2\right). \tag{7}$$

The difference between $T_{\rm av}$ and T_0 reveals itself in terms proportional to the square of the depth of modulation m.

Parametric resonance is possible not only at the frequencies ω_n given in equation (4), but also in ranges of frequencies ω lying on either side of the values ω_n (in the ranges of instability). These intervals become wider as the depth of modulation is increased (see Section 8).

5 The threshold of odd-order parametric resonances

An important difference between parametric excitation and resonance at direct forcing is related to the dependence of the growth of energy on the energy already stored in the system. While for direct forced excitation the increment in energy during one period (at small amplitudes) is proportional to the amplitude of oscillations, i.e., to the square root of the energy, at parametric resonance the increment in energy is proportional to the energy stored in the system.

In conditions of parametric resonance, both the investment in energy caused by the modulation of a parameter and the frictional losses are proportional to the energy stored. Therefore, the parametric resonance is possible only when a threshold is exceeded, that is, when the increment in energy during a period (caused by the parameter variation) is larger than the amount of energy dissipated during the same time. The critical (threshold) value of the modulation depth depends on friction. However, if the threshold is exceeded, the frictional losses of energy cannot restrict the growth of the amplitude. With friction, stationary oscillations of a finite amplitude eventually establish due to nonlinear properties of the pendulum, as we already discussed in Section 3.

We can use arguments employing the conservation laws to evaluate the modulation depth that corresponds to the threshold of parametric excitation. During abrupt radial displacements of the weights, the angular momentum $L = I\omega$ of the pendulum is conserved. Therefore, it is convenient to use the expression $E_{\rm kin} = L^2/(2I)$, which gives the kinetic energy of the pendulum in terms of L and I. For the increment ΔE in the kinetic energy that occurs during an abrupt shift of the weights toward the axis, when the moment of inertia decreases from the value $I_1 = I_0(1+m)$ to the value $I_2 = I_0(1-m)$, we can write:

$$\Delta E = \frac{L^2}{2I_0}\left(\frac{1}{1-m}-\frac{1}{1+m}\right) \approx 2m\frac{L^2}{2I_0} \approx 2mE_{\rm kin}. \tag{8}$$

The approximate expressions in (8) are valid for small values of the modulation depth ($m \ll 1$). If the event occurs near the equilibrium position of the pendulum, when the total energy E of the pendulum is approximately its kinetic energy $E_{\rm kin}$, Eq. (8) shows that the fractional increment in the total energy $\Delta E/E$ approximately equals twice the value of the modulation depth m: $\Delta E/E \approx 2m$.

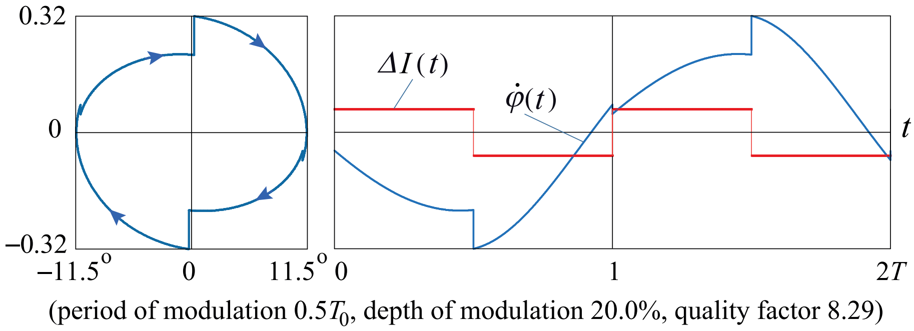

Figure 7: The phase trajectory (left) and the time-dependent graph of the angular velocity $\dot{\varphi}(t)$ (right) for stationary oscillations at the threshold condition $m \approx \pi/2Q$ for $T = T_0/2$.

When the frequencies and phases have those values that are favorable for the most effective delivery of energy, the abrupt outward displacement of the weights occurs at the time moment at which the pendulum attains its greatest deflection (more precisely, when the pendulum is very near it). At this moment the angular velocity of the pendulum is almost zero, and so this radial displacement of the weights into their previous positions causes nearly no decrement in the energy.

For the principal resonance ($n = 1$) the investment in energy occurs twice during the natural period T_0 of oscillations. That is, the fractional increment in energy $\Delta E/E$ during one period approximately equals $4m$.

A process in which the increment in energy ΔE during a period is proportional to the energy stored E (in the case under consideration $\Delta E \approx 4mE$) is characterized on the average by the exponential growth of the energy with time:

$$E(t) = E_0 \exp(\alpha t). \tag{9}$$

In this case the index of growth α is proportional to the depth of modulation m of the moment of inertia: $\alpha = 4m/T_0$. When the modulation is exactly tuned to the principal resonance ($T = T_{av}/2 \approx T_0/2$), the decrease of energy is caused almost only by friction. Dissipation of energy due to viscous friction during an integer number of natural cycles (for $t = nT_0$) is described by the following expression:

$$E(t) = E_0 \exp(-2\gamma t). \tag{10}$$

Comparing Eqs. (9) and (10), we obtain the following approximate estimate for the threshold (minimal) value m_{min} of the depth of modulation corresponding to the excitation of the principal parametric resonance:

$$m_{min} = \frac{1}{2}\gamma T_0 = \frac{\pi}{2Q}. \tag{11}$$

Here we introduced the dimensionless quality factor $Q = \omega_0/(2\gamma)$ to characterize the strength of friction in the system.

The phase trajectory and the plots of time dependence of the angular velocity for parametric oscillations of a small amplitude occurring at the threshold conditions, Eq. (11), are shown in Figure 7. We can see on the graph and on the phase trajectory only abrupt increments in the magnitude of the angular velocity occurring twice during the period of oscillation (when the weights are shifted inward). The outward shifts occur at time moments at which the angular velocity is almost zero. The corresponding decrements in velocity are too small to be clearly visible on the graphs. This mode of oscillations (which have a constant amplitude in spite of the dissipation of energy) is called parametric regeneration.

Computer simulations show that this regime of parametric regeneration is stable with respect to small variations in initial conditions: At different initial conditions the phase trajectory and graphs acquire after a while the same characteristic shape. However, this regime is unstable with respect to variations of the pendulum's parameters. If the friction is slightly greater or the depth of modulation slightly smaller than is required by Eq. (11), oscillations gradually damp in spite of the modulation. Otherwise, the amplitude grows.

For the 3rd-order resonance ($T = 3T_0/2$) the threshold value of the modulation depth is approximately three times greater than its value for the principal resonance: $m_{\min} \approx 3\pi/(2Q)$. In this instance two cycles of the parametric variation occur during three full periods of natural oscillations. Radial displacements of the weights again happen at the time moments most favorable for pumping the pendulum—inward at the equilibrium position, and outward at the extreme positions. The same investment in energy occurs during a lapse of time which is three times longer than for the principal resonance.

6 Amplification and attenuation of oscillations by a feedback

In the above analysis, we assumed that the period T of modulation remains the same as the amplitude increases. At exact tuning to the principal resonance, this period equals $T_{\mathrm{av}}/2$, where T_{av} is the average period of small natural oscillations. As the amplitude grows, the natural period of the pendulum becomes longer, the conditions of resonance become violated, and the drive drifts out of phase with the pendulum.

When we apply the model of the pendulum with modulated length for explaining the pumping of a playground swing, we should take into account that the child on the swing may notice the lengthening of the natural period as the amplitude increases, and can react correspondingly, increasing the period of pumping to stay in phase with the swing. This intuitive reaction may be considered as a kind of feedback loop: The child determines the time moments to squat and to stand depending on the actual position of the swing. For the pendulum with modulated length, this situation was analyzed in [23].

We can include this feedback loop in our model of the physical pendulum with modulated inertia moment, which we explore in the present paper, by requiring that instantaneous inward shifts of the auxiliary weights occur exactly at the time moments, at which the pendulum crosses the equilibrium position, and that backward (outward) shifts occur exactly at extreme positions of the pendulum. Such manipulations correspond to the optimal active control that provides the most effective and rapid pumping of the pendulum (at a given friction and a given value of the modulation depth) with the help of a positive feedback.

Figure 8 shows the graph of progressively growing oscillations occurring under this feedback control. Initially the period of modulation T satisfies conditions of the principal parametric resonance at small swing ($T = T_{\mathrm{av}}/2$). We note how the period T of the square-wave modulation increases due to the feedback as the the amplitude of the pendulum grows. These increments of the modulation period occur in accordance with the growing average natural period of the pendulum. The feedback-driven adaptation to the changed natural frequency corresponds to "walking along the backbone" (or "skeleton") of the frequency response resonance peak for a parametrically excited nonlinear pendulum. After the amplitude reaches $180°$, the pendulum executes full revolutions.

The above-described strategy of oscillations control by varying the key parameter (the moment of inertia) can dramatically amplify the oscillations. No doubt that the priests who pump the suspended incense burner *O Botafumeiro* also use the feedback (maybe intuitively) for controlling the pendulum behavior. They increase gradually the period of modulation to stay in

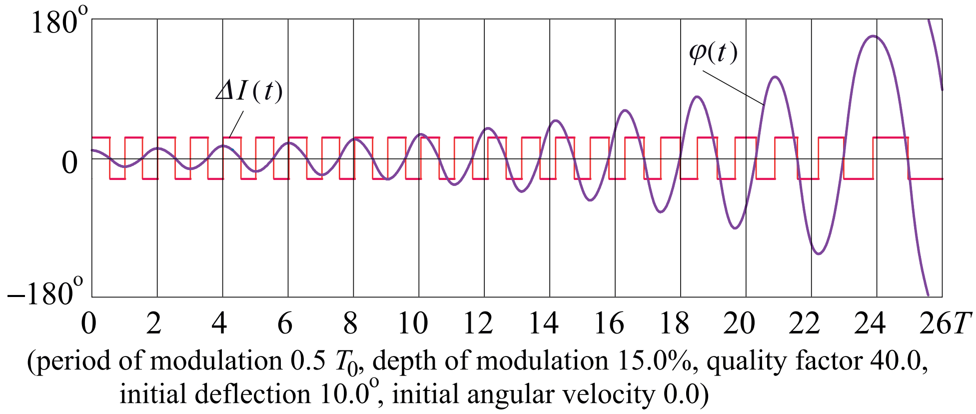

Figure 8: Parametric pumping of the pendulum with the usage of a feedback loop that provides the most effective delivery of energy to the pendulum.

phase with the swinging pendulum as the amplitude grows, and then probably reduce the modulation depth to the level, sufficient to compensate for frictional losses and to maintain the desirable swing.

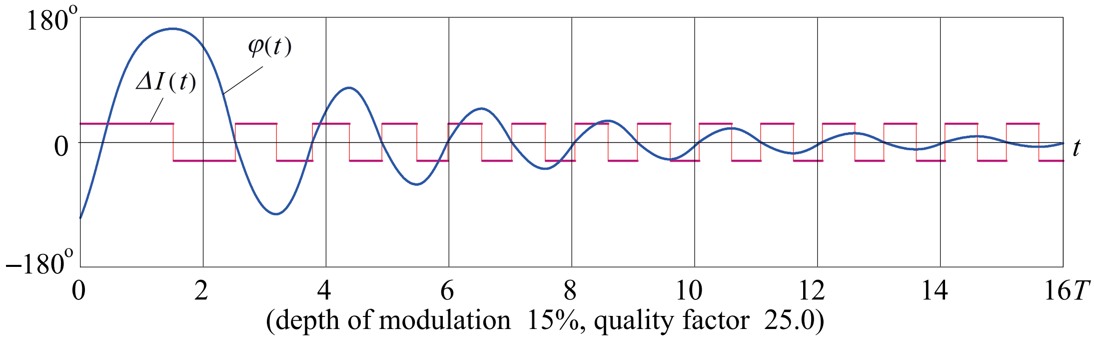

Figure 9: Parametric attenuation of the pendulum swing with the usage of a negative feedback loop that provides the most effective reduction of energy of the pendulum.

The efficient strategy of optimal active control for the most rapid damping of existing oscillations with the usage of a feedback consists in reversing the phase of modulation with respect to above-described method of pumping. Namely, for a successful control scheme the moment of inertia of the pendulum must be increased by shifting the wrights apart at time moments of crossing the equilibrium position, and the moment of inertia must be reduced by shifting the weights inward at extreme positions of the pendulum. Figure 9 illustrates the attenuation of oscillations by the usage of this negative feedback.

Suspended heavy construction beams or plates can be also subject to rotary oscillations about the vertical axis (see Figure 10). Such undesired oscillations can be suppressed by reconfigurations of auxiliary masses whose position influences the central moment of inertia of the suspended body about the vertical axis. Similar control strategy can be realized by using a robot-actuator mounted on a suspended construction: For the most effective attenuation of harmful rotary oscillations, the additional masses must be shifted outward at the instants the suspended body passes through the equilibrium position, and the masses must be shifted inward at the extreme angular displacements of the body.

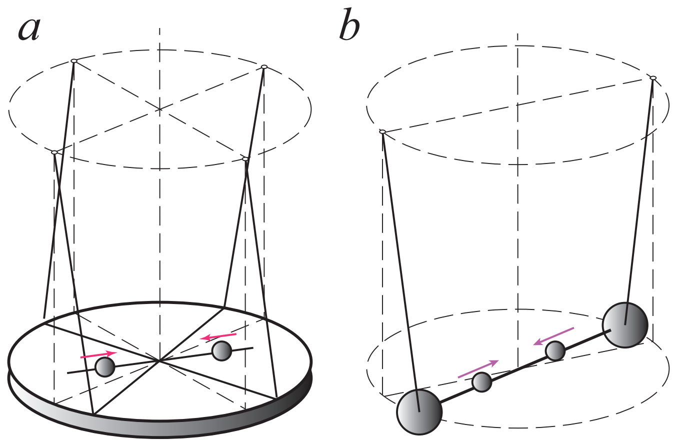

Figure 10: Parametric suppressing by auxiliary masses' reconfigurations of the undesired rotary oscillations of heavy suspended constructions about the vertical axis with the usage of a negative feedback.

7 Phase locking and parametric autoresonance

Using the positive feedback, we can excite large swinging of the pendulum by variations of the parameter at a relatively small excess of the drive over the threshold. But it is also possible to do this without a feedback, that is, without appropriately adjusting the period and phase of modulation during the process of the amplitude growing. It occurs that under certain conditions a spontaneous phase locking between the drive and the pendulum motion becomes possible: The pendulum can automatically adjust its amplitude to stay matched with the drive. By sweeping appropriately the period of modulation, we can control the amplitude of the pendulum. This phenomenon is called parametric autoresonance. Autoresonance allows us to both excite and control a large resonant response in nonlinear systems by a small forcing.

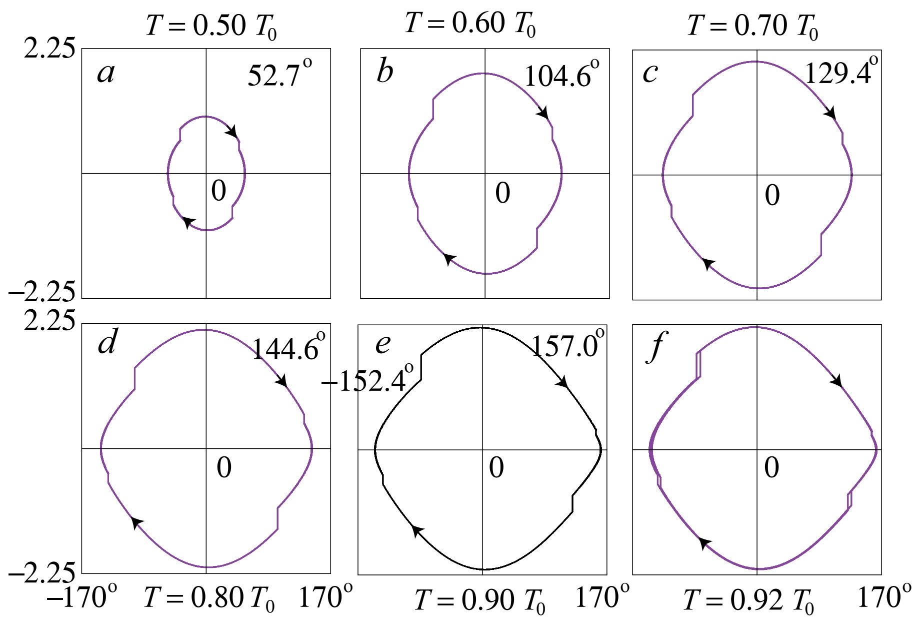

Figure 11: Evolution of the phase trajectory at autoresonance.

We can start pumping the pendulum by modulating its moment of inertia with period $T = T_0/2$, which corresponds to the condition of resonance at an infinitely small swing. Then, in the process of oscillations, we slowly increase the period of modulation. This can be done in small steps. After each small increment of the period, we must wait for a while so that transients almost fade away. During this time, the amplitude increases just to the amount which provides matching of an increased natural period of the pendulum with the new period of modulation. This sweeping corresponds to a slow climbing up the upper slope of the frequency-response peak. In each step of the sweeping, the pendulum remains locked in phase with the drive. The relationship between the current value of the modulation period and the autoresonant amplitude corresponds to the theoretical dependence of the average natural period of the pendulum on the amplitude of its free oscillations.

In order to illustrate the phenomenon of parametric autoresonance in a computer simulation, we choose the following values for the pendulum parameters: Depth of modulation 15%, quality factor $Q = 40$ – a relatively weak friction (for the threshold at $m = 15\%$, according to Eq. (11), $Q \approx 10.5$). At $T = 0.5\,T_0$ the steady-state amplitude equals 52.7°. Phase trajectories for several stages of the autoresonance are shown in Figure 11, $a-f$. This sequence of steady-state phase orbits clearly shows peculiarities of the non-linear system response on slowly increasing period of modulation. When the period of modulation is gradually increased from $T = 0.50\,T_0$ up to $T = 0.80\,T_0$, the steady-state amplitude increases up to 144.6°. Then the symmetry-breaking bifurcation occurs: At $T = 0.90\,T_0$ the pendulum swings to one side through an angle of 152.4° and to the other side – through 157.0° (Figure 11, *e*). Further on, this asymmetry increases: At $T = 0.9190\,T_0$ maximum deflection of the pendulum to one side equals 145.7°, while its excursion to the other side is 163.3°.

The asymmetry of the pendulum oscillations increases up to $T = 0.9195\,T_0$, when the bifurcation of period-doubling occurs: At $T = 0.9200\,T_0$ during two cycles of modulation the

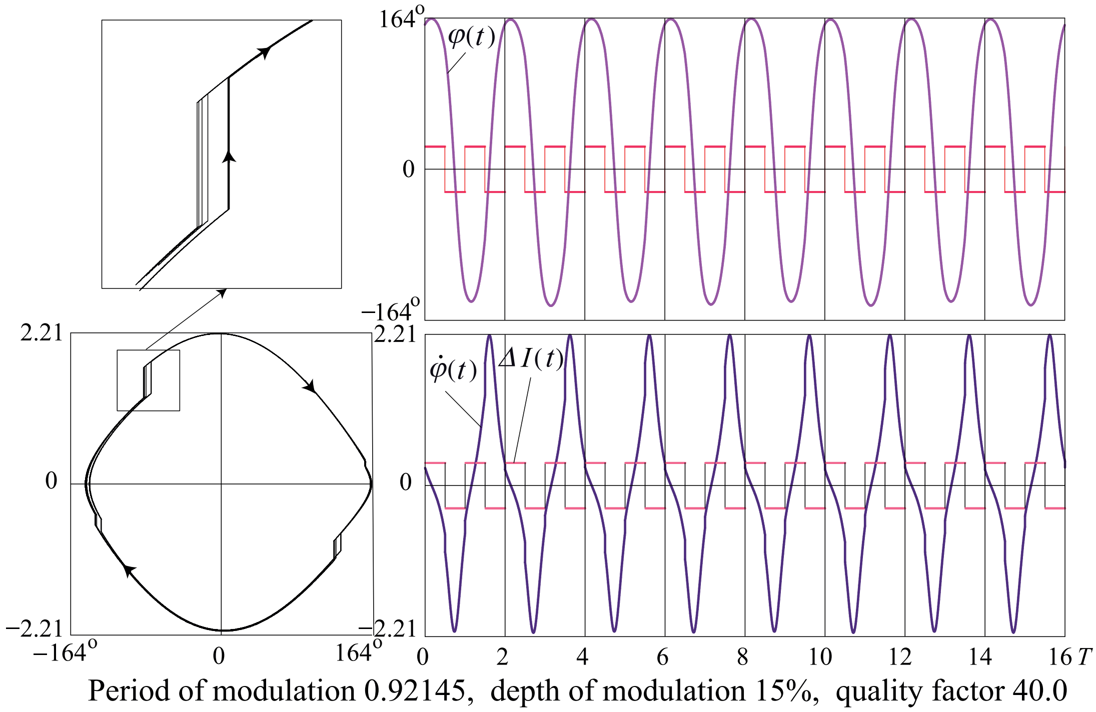

Figure 12: Oscillations at parametric autoresonance, which occur after the bifurcations of symmetry breaking and period doubling.

pendulum executes one asymmetric oscillation between the values 135.8° and 163.2°, while during the next two cycles the pendulum swings between 147.5° and 163.6°. Then the process repeats. Thus, one period of the pendulum motion covers now four periods of excitation (Figure 11, *f*). We note that the closed phase trajectory of this limit cycle is formed by two nearby almost merging loops. Such asymmetric regimes exist (for the same values of *m* and *Q*) in pairs, whose phase orbits are mirror images of one another.

Further increments of the period of modulation by tiny steps causes a whole condensing cascade of nearby period-doubling bifurcations. Figure 12 illustrates the steady-state regime whose period covers 8 cycles of the pendulum with slightly different amplitudes, and lasts 16 cycles of modulation. This cascade of bifurcations ends at $T = 0.92145\,T_0$ by a crisis: Asymmetric oscillations of the pendulum become unstable, occurring with seldom transitions between the two kinds of asymmetry (intermittency). Finally the pendulum turns over the upper equilibrium, and then, after long irregular transient oscillations with gradually diminishing amplitude, eventually comes to rest in the downward vertical position.

Stationary large-amplitude parametric oscillations of the pendulum, locked in phase with the drive and occurring at a small or moderate modulation (like those described above and shown in Figure 12), can be excited not only by slowly sweeping the drive period, but also by choosing appropriate initial conditions. The system eventually comes to a certain periodic regime (limit cycle, or attractor), if initial conditions are chosen within the basin of attraction of this regime. In nonlinear systems different periodic regimes may coexist at the same values of parameters. This property is called multistability.

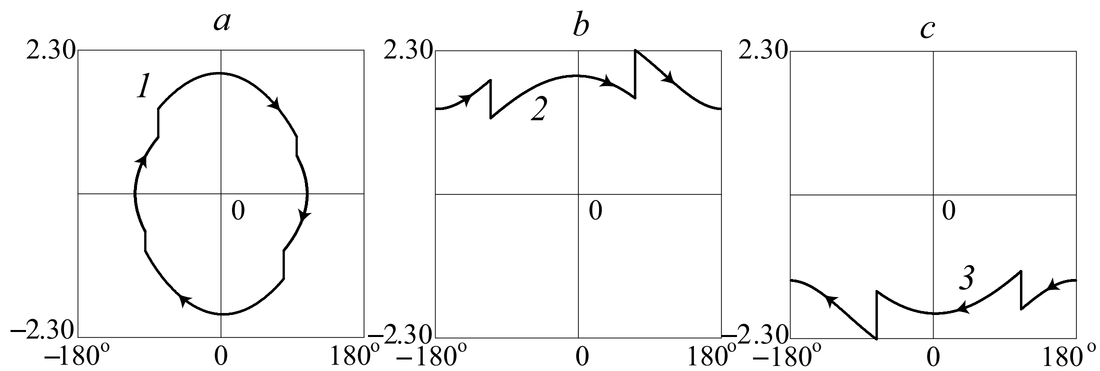

(period of modulation 0.6 T_0, depth of modulation 20%, quality factor 40.0)

Figure 13: Stationary periodic oscillations and rotations of the pendulum, occurring at the same values of the system parameters.

An example of multistability is shown in Figure 13, *a* – *c*. Closed curve *1* (Figure 13, *a*) describes stationary periodic oscillation of the pendulum with a finite amplitude, which corresponds to the principal parametric resonance. One period of these oscillations covers two cycles of excitation. Curves *2* and *3* (Figure 13, *b* – *c*) correspond to period-1 unidirectional rotations of the pendulum in counterclockwise and clockwise directions, respectively. The pendulum makes one revolution during each period of modulation. One more attractor is represented by a single point at the origin of the phase plane, which describes the state of rest of the pendulum in the downward vertical position. Each of these different stationary modes, coexisting at the same values of all parameters of the pendulum and the drive, is characterized by a certain basin of attraction in the phase plane of initial states.

8 Main interval and odd-order intervals of instability

Next we consider a more rigorous mathematical treatment of parametric resonance under square-wave modulation of the parameter, based on the differential equations (2)–(3) that describe the model of the investigated system. At each time moment $t_n = nT/2$ ($n = 1,\ 2,\ \dots$) of an abrupt change in the moment of inertia of the pendulum, we must make a transition from one of the equations (2)–(3) to the other. During each half-period $T/2$ the motion of the pendulum is a segment of some natural oscillation. Analytical solutions that describe the system can be obtained by fitting to one another known solutions to equations (2)–(3) for consecutive adjacent time intervals.

The initial conditions for each subsequent time interval are chosen in the following way. Each initial value of the angular displacement φ equals the value $\varphi(t)$ reached by the pendulum at the end of the preceding time interval. The initial value of the angular velocity $\dot\varphi$ is related to the angular velocity at the end of the preceding time interval by the law of conservation of the angular momentum:

$$(1+m)\dot\varphi_1 = (1-m)\dot\varphi_2. \tag{12}$$

In Eq. (12) $\dot\varphi_1$ is the angular velocity at the end of the preceding time interval, when the moment of inertia of the pendulum has the value $I_1 = I_0(1+m)$, and $\dot\varphi_2$ is the initial value for the following time interval, during which the moment of inertia equals $I_2 = I_0(1-m)$. The change in the angular velocity at an abrupt variation of the inertia moment from the value I_2 to I_1 can be found in the same way. We may use here the conservation of angular momentum, Eq. (12), because at sufficiently rapid displacement of the auxiliary masses across the pendulum, the influence of the torque produced by the force of gravity is negligible. In other words, we can assume the pendulum to be freely rotating about its axis. This assumption is valid provided the duration of the displacement of the masses constitutes a small portion of the natural period.

Considering conditions for which equations (2)–(3) yield solutions with increasing amplitudes, we determine ranges of the period of modulation T near the values $T_n = nT_{\rm av}/2$, within which the state of rest in the equilibrium position is unstable for a given modulation depth m. In these ranges of parametric instability, an arbitrarily small deflection from equilibrium is sufficient for the progressive growth of initially small oscillations.

To find the boundaries of the frequency ranges of parametric instability surrounding the resonant values $T = T_{\rm av}/2$, $T = T_{\rm av}$, $T = 3T_{\rm av}/2,\ \dots$, we can consider that when the period of modulation T corresponds to one of the boundaries of the desired intervals of instability, stationary oscillations occur with an indefinitely small amplitude. Therefore in equations (2)–(3) we can replace the sine functions of the deflection angle by their arguments.

For the principal resonance, the period of modulation T equals $T_{\rm av}/2$ (one half the average natural period), which means that twice during the full cycle of natural oscillation of the pendulum the angular velocity abruptly increases, and twice it decreases (see Figure 14). The increments in velocity are greater than the decrements, so that as a whole the energy received by the pendulum exceeds the energy given away. This surplus of the energy compensates for the dissipation of the energy which occurs in the motion during the intervals between the abrupt displacements of the additional weights. These periodic stationary oscillations can be represented as an alternation of natural oscillations of the pendulum with the periods T_1 and T_2.

To find conditions at which such stationary oscillations take place, we can write the expressions for $\varphi(t)$ and $\dot\varphi(t)$ during the adjacent intervals when the pendulum executes damped natural oscillations, and then fit these expressions to one another at the boundaries. Such fitting must provide a periodic stationary process. We choose as the time origin $t = 0$ the instant when the weights are shifted apart, and the angular velocity is decreased in magnitude. Then during the interval $(0,\ T/2)$ the graph describes a damped natural oscillation with the frequency

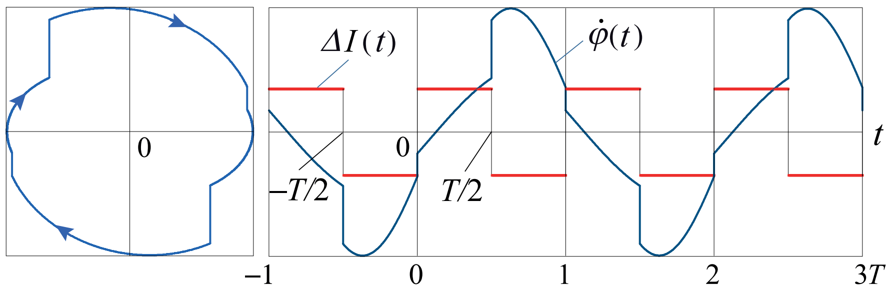

Depth of modulation 35%, period of modulation $0.43T_0$, quality 8.95

Figure 14: Phase trajectory and time-dependent graphs of stationary parametric oscillations at the lower boundary of the principal interval of instability (near $T = T_{av}/2$).

$\omega_1 = \omega_0/\sqrt{1+m}$. It is convenient to represent this motion as a superposition of natural damped oscillations of sine and cosine type with some constants A_1 and B_1:

$$\begin{aligned} \varphi_1(t) = &\quad (A_1 \sin\omega_1 t + B_1 \cos\omega_1 t)\, e^{-\gamma t}, \\ \dot\varphi_1(t) \approx &\quad (A_1\omega_1 \cos\omega_1 t - B_1\omega_1 \sin\omega_1 t)\, e^{-\gamma t}. \end{aligned} \tag{13}$$

The latter expression for $\dot\varphi(t)$ is valid for relatively weak friction ($\gamma \ll \omega_0$). To obtain it, we differentiate $\varphi(t)$ with respect to the time, considering the exponential factor $e^{-\gamma t}$ to be approximately constant. Indeed, at weak damping the main contribution to the time derivative originates from the oscillating factors $\sin\omega_1 t$ and $\cos\omega_1 t$ in the expression for $\varphi(t)$. Similarly, during the interval $(-T/2,\ 0)$ the graph in Figure 14 is a segment of damped natural oscillation with the frequency ω_2:

$$\begin{aligned} \varphi_2(t) = &\quad (A_2 \sin\omega_2 t + B_2 \cos\omega_2 t)\, e^{-\gamma t}, \\ \dot\varphi_2(t) \approx &\quad (A_2\omega_2 \cos\omega_2 t - B_2\omega_2 \sin\omega_2 t)\, e^{-\gamma t}. \end{aligned} \tag{14}$$

To determine the values of constants A_1, A_2, and B_1, B_2, we use the conditions that must be satisfied when the segments of the graph are joined together, and take into account the periodicity of the stationary process. At $t = 0$ the angle of deflection is the same for both φ_1 and φ_2, that is, $\varphi_1(0) = \varphi_2(0)$. From this condition we get $B_2 = B_1$. We later denote these equal constants by B. The angular velocity at $t = 0$ undergoes a sudden change, which follows from the conservation of angular momentum: $(1+m)\dot\varphi_1 = (1-m)\dot\varphi_2$, see Eq. (12). This condition gives us the following relation between A_1 and A_2: $A_2 = hA_1 = hA$ (further on we denote A_1 as A), where we have introduced a dimensionless factor h, which depends on the depth of modulation m:

$$h = \sqrt{\frac{1+m}{1-m}}. \tag{15}$$

For stationary periodic oscillations, corresponding to the principal resonance, as well as to all resonances of odd orders $n = 1,\ 3,\ \ldots$ in Eq. (6), the following conditions of periodicity for φ and $\dot\varphi$ must fulfil:

$$\varphi_1(T/2) = -\varphi_2(-T/2), \quad (1+m)\dot\varphi_1(T/2) = -(1-m)\dot\varphi_2(-T/2). \tag{16}$$

Substituting φ and $\dot\varphi$ in Eq. (16), we obtain the system of homogeneous equations for unknown quantities A and B:

$$\begin{aligned} (pS_1 - hS_2)A + (pC_1 + C_2)B = &\quad 0, \\ h(pC_1 + C_2)A - (phS_1 - S_2)B = &\quad 0, \end{aligned} \tag{17}$$

where $p = \exp(-\gamma T)$. In Eq. (17), the following notations are used:

$$C_1 = \cos(\omega_1 T/2), \qquad C_2 = \cos(\omega_2 T/2),$$
$$S_1 = \sin(\omega_1 T/2), \qquad S_2 = \sin(\omega_2 T/2). \tag{18}$$

The homogeneous system of Eqs. (17) for A and B has a non-trivial (non-zero) solution only if its determinant is zero:

$$2hC_1C_2 - (1+h^2)S_1S_2 + h(p+1/p) = 0. \tag{19}$$

This condition for the existence of a non-zero solution to Eqs. (17) gives us an equation for the unknown variable T, which enters Eq. (19) as the arguments of sine and cosine functions in S_1, S_2 and C_1, C_2, and also as the argument of the exponent in $p = e^{-\gamma T}$. The desired boundaries of the interval of instability T_- and T_+ are given by the roots of the Eq. (19). To find approximate solutions T to this transcendental equation, we transform it into a more convenient form. We first represent in Eq. (19) the products C_1C_2 and S_1S_2 as follows:

$$C_1C_2 = \frac{1}{2}(\cos\frac{\Delta\omega T}{2} + \cos\omega_{\text{av}}T), \quad S_1S_2 = \frac{1}{2}(\cos\frac{\Delta\omega T}{2} - \cos\omega_{\text{av}}T), \tag{20}$$

Then, using the identity $\cos\alpha = 2\cos^2(\alpha/2) - 1$, we reduce equation (19) to the following form:

$$(h+1)\cos(\omega_{\text{av}}T/2) = \pm\sqrt{(h-1)^2\cos^2(\Delta\omega T/4) - h(p+1/p-2)}. \tag{21}$$

To find the boundaries of the interval which contains the principal resonance, we should search for a solution T of Eq. (21) in the vicinity of $T = T_{\text{av}}/2 \approx T_0/2$. If for a given value of the quality factor Q (Q enters $p = e^{-\gamma T}$) the depth of modulation m exceeds the threshold value, Eq. (21) has two solutions which correspond to the desirable boundaries T_- and T_+ of the instability interval. These solutions exist if the expression under the radical sign in Eq. (21) is positive. Its zero value corresponds to the threshold conditions:

$$\frac{(h-1)^2}{h}\cos^2(\Delta\omega T/4) = p + \frac{1}{p} - 2. \tag{22}$$

To evaluate the threshold value of Q for small values of the modulation depth $m \ll 1$, we may assume here $h \approx 1+m$ (see Eq. (15)), and $\cos(\Delta\omega T/4) \approx 1$. On the right-hand side of Eq. (22), in $p = e^{-\gamma T}$, we can consider $\gamma T \approx \gamma T_0/2 = \pi/(2Q) \ll 1$, so that $p + 1/p - 2 \approx (\gamma T)^2 = (\pi/2Q)^2$. Thus, for the threshold of the principal parametric resonance we get the following approximate expression:

$$Q_{\min} \approx \frac{\pi}{2m}, \qquad (m)_{\min} \approx \frac{\pi}{2Q}. \tag{23}$$

This expression for the threshold of main resonance coincides with Eq. (11), obtained earlier from a simple analysis based on the energy considerations.

At the threshold the expression under the radical sign in Eq. (21) is zero. Both its roots (the boundaries of the instability interval) merge. This occurs when the cosine on the left-hand side of Eq. (21) is zero, that is, when its argument equals $\pi/2$:

$$\omega_{\text{av}}\frac{T}{2} = \frac{\pi}{2}, \qquad \text{or} \qquad T = \frac{\pi}{\omega_{\text{av}}} = \frac{1}{2}T_{\text{av}},$$

so that the threshold conditions (23) correspond to exact tuning to resonance, when $T = T_{\text{av}}/2$.

To find numerically the boundaries T_- and T_+ of the instability interval, we represent T in the argument of the cosine function on the left-hand side of Eq. (21) as $T_{\rm av}/2+\Delta T$. Since $\omega_{\rm av}T_{\rm av}=2\pi$, we can express this cosine in the form $-\sin(\omega_{\rm av}\Delta T/2)$. Then Eq. (21) becomes:

$$\sin(\omega_{\rm av}\Delta T/2) = \mp\frac{1}{h+1}\sqrt{(h-1)^2\cos^2\frac{\Delta\omega(\frac{1}{2}T_{\rm av}+\Delta T)}{4} - h\frac{(p-1)^2}{p}}. \qquad (24)$$

This equation for the unknown quantity ΔT can be solved numerically by iteration. We start with $\Delta T=0$ as an approximation of the zeroth order, substituting it into the right-hand side of Eq. (24). Then, the left-hand side of Eq. (24) gives us the values of ΔT for both boundaries of the interval of instability to the first order. We substitute these first-order values into the right-hand side of Eq. (24), and on the left-hand side we obtain ΔT to the second order. This procedure is iterated until a self-consistent values of ΔT for both boundaries are obtained. Performing such calculations for various (arbitrarily large) values of the modulation depth m, we obtain the whole boundaries $T_-(m)$ and $T_+(m)$ for the first interval of parametric instability. Below we explain how the boundaries of other intervals can be calculated.

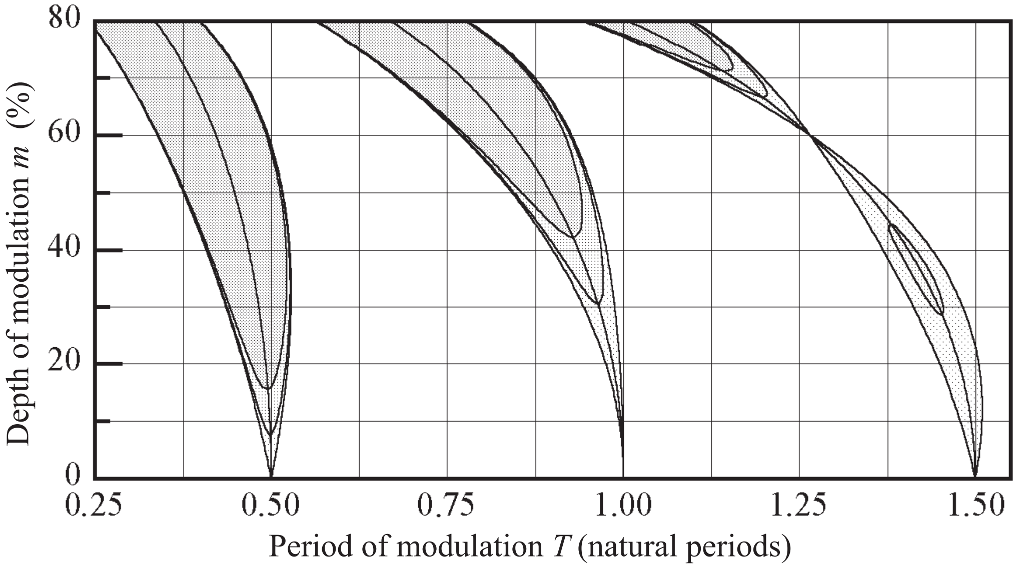

Figure 15: Intervals of parametric instability at square-wave modulation of the pendulum's moment of inertia in the absence of friction, for $Q=20$, and for $Q=10$.

The periods of modulation T_- and T_+ corresponding respectively to the left and right boundaries of the instability interval which contains the principal parametric resonance $n=1$, calculated numerically for different vales of the modulation depth m with the help of the above described procedure, are shown by the first "tongue" in Figure 15. The central curve of this "tongue" gives the period of modulation $T=T_{\rm av}/2$ as a function of the modulation depth m, which corresponds to exact tuning to the principal parametric resonance. The other "tongues" in Figure 15 show the intervals of parametric instability of high orders. Boundaries of the instability for intervals of higher odd orders $n=3,5,\ldots$ are calculated similarly by representing T in Eq.(21) as $nT_{\rm av}/2+\Delta T$, as we explain below. These boundaries are also shown in Figure 15 for several values of the quality factor Q. Intervals of even orders are discussed in Section 9.

The boundaries of the instability interval of the 3rd order can be found in a similar way. At this resonance ($n=3$) two cycles of variation of the inertia moment occur during approximately three natural periods of the pendulum ($T\approx 3T_{\rm av}/2$). The phase trajectories and the time-dependent graphs of small stationary oscillations at the left and right boundaries of the 3rd interval in the absence of friction are shown in Figure 16.

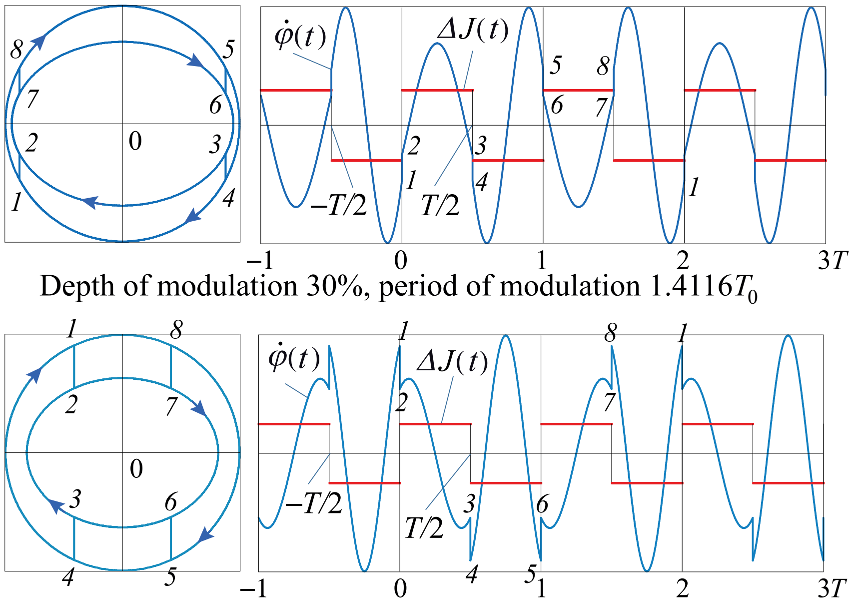

Figure 16: The phase trajectories (left) and the time-dependent graphs of the angular velocity (right) of small stationary parametric oscillations at the left (upper panel) and right (lower panel) boundaries of the interval of instability near $T = 3T_{\rm av}/2$.

The phase orbit of the periodic oscillation closes after two cycles of modulation. This orbit is formed by two concentric ellipses which correspond to small natural oscillations of the pendulum with frequencies ω_1 and ω_2. The representative point moves clockwise along this orbit, jumping from one ellipse to the other each time the weights are abruptly shifted. The numbers in Figure 16 make easier following how the representative point describes this orbit—equivalent points of the phase orbit and the graph of the angular velocity are marked by equal numbers.

Considering conditions at which the graphs of natural oscillations with frequencies ω_1 and ω_2 fit one another for adjacent time intervals of the square-wave modulation and produce the periodic process shown in Figure 16, we get the same Eqs. (17) for A and B, as well as Eq. (21) for the period of modulation. Actually, this is true for all intervals of parametric instability of odd orders. If we are interested in the 3rd interval, we should search for a solution to these equations in the vicinity of $T = 3T_{\rm av}/2$, as well as for any other interval of odd order n—in the vicinity of $T = nT_{\rm av}/2$. The boundaries of intervals of the 3rd order, obtained by a numerical solution of Eq. (21), are also shown in Figure 15.

To obtain approximate analytical solutions to Eq. (21) that are valid for small values of the modulation depth m, we can simplify the expression on the right-hand side of Eq. (21) by assuming that $h \approx 1+m$, $h-1 \approx m$. We may also assume the value of the cosine to be approximately 1. On the left-hand side of Eq. (21), the sine can be replaced by its small argument, in which $\omega_{\rm av} = 2\pi/T_{\rm av}$. This yields the following approximate expressions for both boundaries of the main interval that are valid up to terms to the second order in $m \ll 1$:

$$T_{\mp} = \frac{1}{2}\left(1 \mp \frac{m}{\pi}\right) T_{\rm av} = \frac{1}{2}\left(1 \mp \frac{m}{\pi} - \frac{3m^2}{8}\right) T_0. \qquad (25)$$

In this approximation the boundaries of the 3rd interval are given by the following analytical expressions:

$$T_{\mp} = \frac{3}{2}\left(1 \mp \frac{m}{3\pi}\right) T_{\mathrm{av}} = \frac{3}{2}\left(1 \mp \frac{m}{3\pi} - \frac{3m^2}{8}\right) T_0. \tag{26}$$

The 3rd interval has approximately the same width $(m/\pi)T_0$ as does the interval of instability in the vicinity of the principal resonance. However, the 3rd interval is distinguished by greater asymmetry: Its central point is displaced to the left from the value $T = \frac{3}{2}T_0$ by $\frac{9}{16}m^2 T_0$.

Boundaries of the first five intervals of parametric instability in the absence of friction are shown in Figure 17. The instability domains on this diagram are analogues to the well-known Arnold tongues for Mathieu's equation (Ince–Strutt diagram) that describes, in particular, the pendulum, parametrically excited by vertical oscillations of the suspension point.

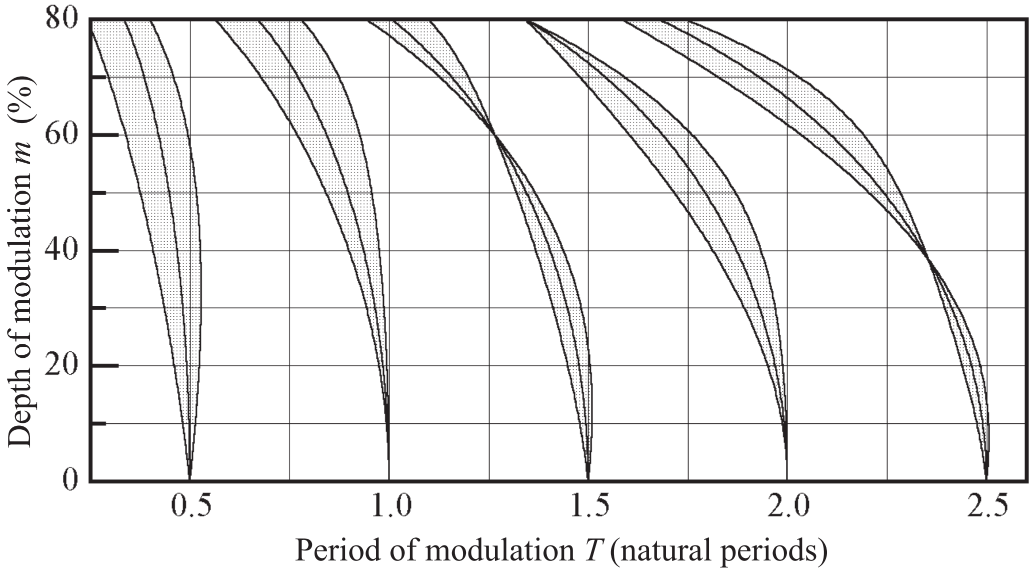

Figure 17: Intervals of parametric instability at square-wave modulation of the inertia moment in the absence of friction.

9 Parametric resonances of even orders

For small and moderate square-wave modulation of the moment of inertia, parametric resonance of the order $n = 2$ (one cycle of the modulation during one natural period of oscillation) is relatively weak compared to the above considered resonances $n = 1$ and $n = 3$. Indeed, for $n = 2$ the abrupt shifts of the auxiliary masses induce both an increase and a decrease of the energy only once during each natural period. The growth of oscillations occurs only if the weights are shifted inward when the angular velocity of the pendulum is greater in magnitude than it is when the weights are shifted outward. For $T \approx T_{\mathrm{av}}$, these conditions can fulfill only by virtue of a (small) difference between the natural periods T_1 and T_2 of the pendulum. This difference in the natural periods is proportional to m.

The growth of oscillations at parametric resonance of the 2nd order is shown in Figure 18. We note the asymmetric character of oscillations at $n = 2$ resonance: The angular excursion of the pendulum to one side is greater than to the other. The investment in energy during a period is proportional to the square of the depth of modulation m, while for resonances with $n = 1$ and

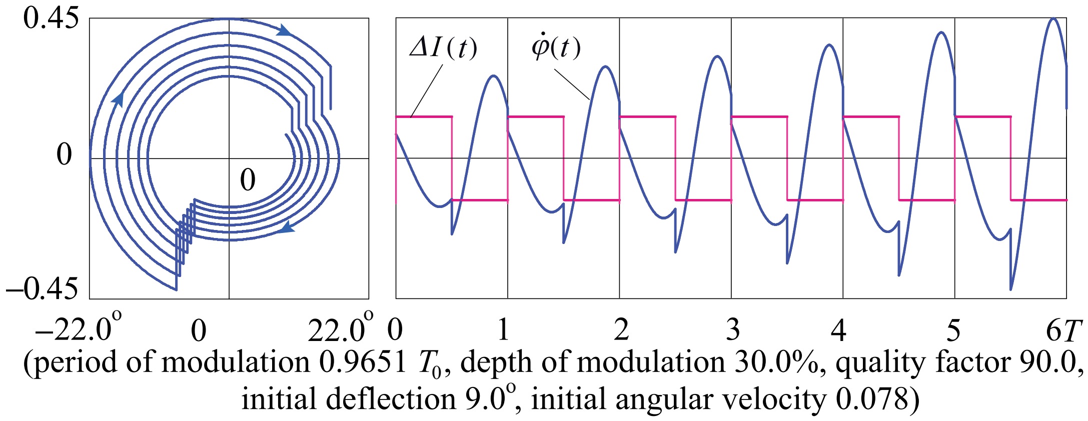

Figure 18: The phase trajectory and the graphs of angular velocity $\dot{\varphi}(t)$ of oscillations corresponding to parametric resonance of the 2nd order $n = 2$ ($T \approx T_{av}$).

$n = 3$ the investment in energy is proportional to the first power of m. Therefore, for the same value of the damping constant γ (the same quality factor Q), a considerably greater depth of modulation is required here to exceed the threshold of excitation. The growth of the amplitude again is restricted by the nonlinear properties of the pendulum. The interval of instability in the vicinity of $n = 2$ resonance (for small values of m) is considerably narrower compared to the corresponding intervals of $n = 1$ and $n = 3$ resonances. Its width is also proportional only to the square of m.

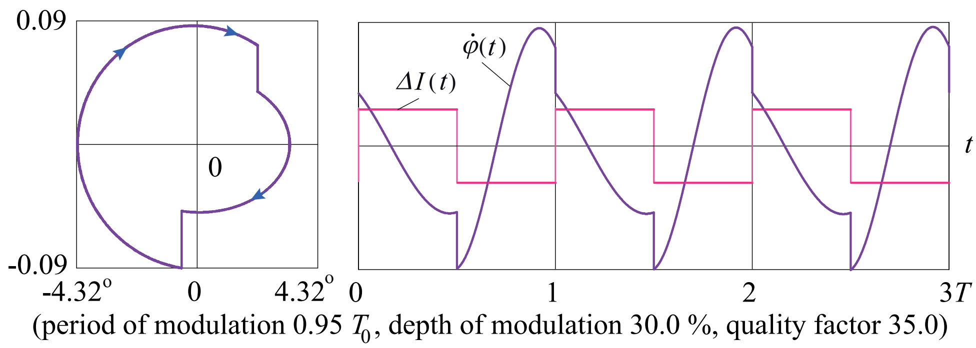

Figure 19: The phase trajectory and the time-dependent graph of angular velocity $\dot{\varphi}(t)$ of stationary parametric oscillations at the lower boundary of the 2nd interval of instability (near $T = T_{av}$).

To determine the boundaries of this interval of instability, we can consider, as is done above for resonances of odd orders, small stationary oscillations for $T \approx T_0$ formed by alternating segments of free damped oscillations with the periods T_1 and T_2 (see Figure 19). Fitting these segments for the adjacent half-cycles of modulation, we arrive to the following equation for the boundaries of the 2nd interval of parametric instability:

$$(1+h)\sin\omega_{av}\frac{T}{2} = \pm\sqrt{(1-h)^2\sin^2(\Delta\omega T/4) - h(p+1/p-2)}. \tag{27}$$

We should search for its solution T in the vicinity of $T = T_0 \approx T_{av}$. If the depth of modulation m exceeds the threshold value for a given value of the quality factor Q (the quantity $p = e^{-\gamma T}$ in the above equation depends on Q), Eq. (27) has two solutions which correspond to the boundaries T_- and T_+ of the instability interval. These solutions exist if the expression under the radical sign in Eq. (27) is positive. Its zero value corresponds to the threshold conditions:

$$\frac{(h-1)^2}{h}\sin^2(\Delta\omega T_{\rm av}/4) = \frac{(p-1)^2}{p}. \qquad (28)$$

To estimate the threshold value of Q for small values of the modulation depth m, we may assume here $h \approx 1+m$, and $\sin(\Delta\omega T/4) \approx \Delta\omega T/4$. In the right-hand side of Eq. (28), in $p = e^{-\gamma T}$, we can consider $\gamma T \approx \gamma T_0 = \pi/Q \ll 1$, so that $p + 1/p - 2 = (p-1)^2/p \approx (\gamma T)^2 = (\pi/Q)^2$. Thus, for the threshold of the 2nd parametric resonance we obtain:

$$Q_{\rm min} \approx \frac{2}{m^2}, \qquad m_{\rm min} \approx \sqrt{\frac{2}{Q}}. \qquad (29)$$

The threshold conditions correspond to exact tuning to resonance, when $T = T_{\rm av}$.

To find the boundaries T_- and T_+ of the 2nd instability interval, we represent T in the argument of the sine function in the left-hand side of Eq. (27) as $T_{\rm av} + \Delta T$, where $\Delta T \ll T_{\rm av} \approx T_0$. Since $\omega_{\rm av} T_{\rm av} = 2\pi$, we can write this sine as $-\sin(\omega_{\rm av}\Delta T/2)$. Then Eq. (27) becomes:

$$\sin\frac{\omega_{\rm av}\Delta T}{2} = \mp\frac{1}{1+h}\sqrt{(h-1)^2\sin^2\frac{\Delta\omega(T_{\rm av}+\Delta T)}{4} - h\frac{(p-1)^2}{p}}. \qquad (30)$$

This form of the equation is convenient for numerical solution by iteration. The boundaries of the 2nd interval of parametric instability are shown on the diagrams in Figures 15 and 17 together with intervals of higher odd and even orders, which are obtained with the help of similar numeric calculations.

We note how the intervals of even resonances (n =2, 4, 6) are narrow at small values of the modulation depth m in contrast to the intervals of odd orders. The physical reason for this difference was already explained above, at the very beginning of this section. With the growth of the modulation depth m the even intervals expand and become comparable with the intervals of odd orders.

To obtain an approximate solution of Eq. (30), valid for small values of the modulation depth m up to the terms of the second order of m, we can simplify the expression under the radical sign in the right-hand side of Eq. (30), assuming $h \approx 1+m$, $(1-h)^2 \approx m^2$, and $\sin\Delta\omega(T_{\rm av}+\Delta T)/4 \approx \Delta\omega T_{\rm av}$. The last term of the radicand can be represented as $(2/Q)^2 \approx m_{\rm min}^4$. In the left-hand side the sine can be replaced by its small argument, in which $\omega_{\rm av} = 2\pi/T_{\rm av}$. Thus for the boundaries of the second instability interval we obtain the following approximate expressions:

$$\frac{\Delta T}{T_{\rm av}} \approx \mp\frac{1}{4}\sqrt{m^4 - m_{\rm min}^4}, \quad \text{or} \quad T_{\mp} = \left(1 \mp \frac{1}{4}\sqrt{m^4 - m_{\rm min}^4}\right) T_{\rm av}. \qquad (31)$$

In the presence of friction, for a given value m of the depth of square-wave modulation, only several first intervals of parametric resonance can exist (the corresponding "tongues" of instability appear only if m exceeds the threshold value), in contrast to the idealized case of zero friction (see the diagram in Figure 15). We note the "island" of parametric resonance for $n = 3$ and $Q = 20$. This resonance disappears when the depth of modulation exceeds 45% and reappears when m exceeds approximately 66%.

10 Intersections of the boundaries at large modulation

Figure 17 shows that at certain values of m both boundaries of intervals with $n > 2$ coincide (we may consider that these boundaries intersect). This means that at these values of m the corresponding intervals of parametric instability disappear. Such values of m correspond to the natural periods of oscillation T_1 and T_2, whose ratio is 2 : 1, 3 : 1, and 3 : 2. Next we give a physical explanation for such disappearing of the instability intervals.

For the first of these intersections (ratio $T_1 : T_2 = 2 : 1$) exactly one half of the natural oscillation with period T_1 is completed during the first half of the modulation cycle (see Figure 20). On the phase diagram, the representing point traces a half of the smaller ellipse (*1* — *2*), and then abruptly jumps down to the larger ellipse (*2* — *3*).

During the second half of the modulation cycle the pendulum executes exactly a whole natural oscillation with the corresponding period $T_2 = T_1/2$, so that the representing point passes in the phase plane along the whole larger ellipse (*3* — *4*), and then jumps up to the smaller ellipse along the same vertical segment (*4* — *5*).

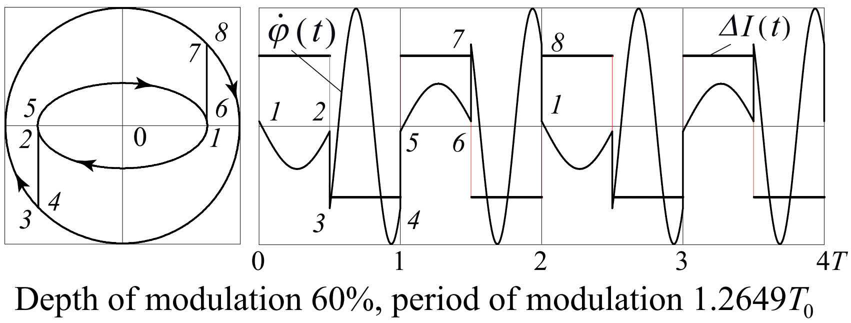

Figure 20: The phase trajectory and time-dependent graphs of angular velocity $\dot{\varphi}(t)$ for stationary oscillations at the intersection of both boundaries of the 3rd interval.

During the next modulation cycle, the representing point generates first the other half of the smaller ellipse (*5* — *6*), and then again the whole larger ellipse (*7* — *8*). Therefore, during any two adjacent cycles of modulation the representing point passes once along the closed smaller ellipse and twice along the larger one, returning finally to the initial point of the phase plane.

We see that such an oscillation, occurring at an intersection of the boundaries of the instability interval, is periodic for arbitrary initial conditions. This means that for the corresponding values of the modulation depth m and the period of modulation T the growth of amplitude is impossible even in the absence of friction (the instability interval vanishes).

Similar explanations can be suggested for other cases in Figure 17 in which the boundaries of the instability intervals intersect.

11 Concluding discussion

We have shown in this paper that a physical pendulum whose moment of inertia is subject to square-wave modulation by a redistribution of auxiliary masses gives a very convenient example in which the phenomenon of parametric resonance in a nonlinear system can be clearly explained with all its peculiarities directly on the basis of the fundamental laws of physics. The threshold of parametric excitation of a nonlinear system in the presence of friction is easily determined on the basis of energy considerations. The boundaries of parametric instability ranges are found quantitatively by rigorous physically transparent mathematical means, without the usage of the Floquet theory, infinite Hill's determinants and perturbation technique. The method is based on fitting the analytical solutions that correspond to adjacent time intervals, during which the moment of inertia is constant.

In a linear system, if the threshold of parametric excitation is exceeded, the amplitude of parametrically excited oscillations increases without limit exponentially with time. In contrast to oscillations at direct forcing, linear viscous friction is unable to restrict the growth of the amplitude at parametric resonance. In real systems like the pendulum the growth of the amplitude is restricted by nonlinear effects that cause the natural period of the system to depend on the amplitude. During parametric excitation the growth of the amplitude leads to an increment in the natural period of the pendulum. The system slips out of resonance, the swing becomes smaller, and conditions of resonance gradually restore. These transient beats fade out due to friction, and oscillations of a finite amplitude eventually establish.

It is possible to parametrically excite oscillations of a large amplitude in a nonlinear system at a relatively small excess of the drive over the threshold with the help of autoresonance. By increasing slowly the period of modulation during the continuing process of oscillations, we can ensure a spontaneous phase locking between the drive and the pendulum motion. Such autoresonance provides a means to both excite and control large resonant responses in nonlinear systems by a small forcing.

Deliberate variations of the system parameters can ensure an efficient control of oscillations. Positive feedback provides the most rapid growth of oscillations. Undesirable or harmful oscillations of suspended constructions can be robustly suppressed by variations of the moment of inertia controlled by a loop of negative feedback.

Computer simulations aid substantially in understanding the peculiarities of parametric resonance. Visualizing time histories and phase orbits, they show clearly how, over the threshold, restriction of the amplitude growth is caused by nonlinear properties of the system. The simulations illustrate the phenomenon of parametric autoresonance, various periodic oscillatory and rotational regimes that are possible due to the phase locking between the drive and the pendulum. The simulations reveal also bifurcations of symmetry breaking and intriguing sequences of period doubling, complementing thus the analytical investigation in a manner that is mutually reinforcing.

References

[1] Ali H. Nayfeh, Dean T. Mook, Nonlinear Oscillations, Wiley (1995).

[2] H. W. Broer, I. Hoveijn, M. van Noort, C. Simó, G. Vegter, The Parametrically Forced Pendulum: A Case Study in $1\frac{1}{2}$ Degree of Freedom, J. Dynamics and Differential Equations, **16** (2004) 897–947.

[3] E. I. Butikov, On the dynamic stabilization of an inverted pendulum, Am. J. Phys. **69** (2001) 755–768.

[4] E. I. Butikov, Subharmonic Resonances of the Parametrically Driven Pendulum, J. Phys. A: Math. and Gen. **35** (2002) 6209–6231.

[5] E. I. Butikov, Regular and Chaotic Motions of the Parametrically Forced Pendulum: Theory and Simulations, in: Computational Science – ICCS 2002 Springer Verlag, 2002, LNCS 2331 (2009) pp. 1154–1169..

[6] E. I. Butikov, An improved criterion for Kapitza's pendulum stability, J. Phys. A: Math. and Theor. **44** (2011), 295202 (16 pp).

[7] S. M. Curry, How children swing, Am. J. Phys. **44** (1976) 924–926.

[8] P.L. Tea Jr., H.Falk, Pumping on a swing, Am. J. Phys. **36** (1968) 1165–1166 .

[9] W. Case, The pumping of a swing from the standing position, Am. J. Phys. **64** (1996) 215–220.

[10] M. A. Pinsky, A. A. Zevin, Oscillations of a pendulum with a periodically varying length and a model of swing, Int. J. Non-Linear Mech. **34** (1999) 105–109.

[11] A. O. Belyakov, A. P. Seyranian, A. Luongo, Dynamics of the pendulum with periodically varying length, Physica D **238** (2009) 1589–1597.

[12] D. Stilling, W. Szyskowski, Controlling angular oscillations through mass reconfiguration: a variable length pendulum case, Int. J. Non-Linear Mech. **37** (2002) 89–99.

[13] A. P. Seyranian, The Swing: Parametric Resonance. Journal of applied mathematics and mechanics **68** (2004) 757–764.

[14] G. L. Baker, J. A. Blackburn, The Pendulum: A Case Study in Physics, Oxford University Press, 2005.

[15] Juan R. Sanmartin, O Botafumeiro: Parametric pumping in the Middle Ages, Am. J. Phys. **52** (1984) 937–945.

[16] E. I. Butikov, Parametric resonance, Comput. Sci. Eng. (1999) 76–83.

[17] C. Cattani, A.P. Seyranian, The regions of instability of a system with a periodically varying moment of inertia, Journal of Applied Mathematics and Mechanics, **69** (2005), 810–815.

[18] E. I. Butikov, Parametric excitation of a linear oscillator, Eur. J. Phys. **25** (2004) 535–554.

[19] E. I. Butikov, Parametric resonance in a linear oscillator at square-wave modulation, Eur. J. Phys. **26** (2005) 157–174.

[20] L. D. Landau and E. M. Lifschitz, *Mechanics*, Moscow: Fizmatlit (1958) (in Russian).

[21] L. D. Landau and E. M. Lifschitz, *Mechanics*, New York: Pergamon (1976).

[22] Kang-Hun Ahn, Hee Chul Park, Jan Wiersig, and Jongbae Hong, Current Rectification by Spontaneous Symmetry Breaking in Coupled Nanomechanical Shuttles, Phys. Rev. Lett. **97**, 216804 (2006).

[23] E.I. Butikov, Pendulum with a square-wave modulated length, International Journal of Non-Linear Mechanics, **55** (2013), 25–34.